IJIE

UTHM Penerbit
Universiti Tun Hussein Onn Malaysia

INTERNATIONAL JOURNAL OF INTEGRATED ENGINEERING
ISSN: 2229-838X e-ISSN: 2600-7916

Vol. 18 No. 1 (2026) 59-71
https://publisher.uthm.edu.my/ojs/index.php/ijie

Design of Fourth Order Gm-C Low-Pass Filter for Microsensor Readout

Pugazhenthi R[1], Ananiah Durai S[1]*, Nabihah Ahmad[2]

[1] *Centre for Nanoelectronics and VLSI Design*
Vellore institution of technology, Chennai, 600127, INDIA
[2] *VLSI and Embedded System Technology (VEST) Focus Group, Faculty of Electrical and Electronic Engineering, Universiti Tun Hussein Onn Malaysia, 86400, Parit Raja, Johor, MALAYSIA*

*Corresponding Author: ananiahdurai.s@vit.ac.in
DOI: https://doi.org/10.30880/ijie.2026.18.01.005

Article Info

Received: 12 December 2025
Accepted: 28 March 2025
Available online: 17 April 2026

Keywords

CMOS technology, passband ripples, signal conditioning, Gm-C filter, low-pass filter, gain error, steep roll-off

Abstract

This paper presents the design and implementation of a fourth-order transconductance-capacitance (Gm-C) low-pass filter for signal conditioning in interface electronics, realized in gpdk 90 nm CMOS technology. The proposed filter employs a tunable OTA-based multi-stage architecture to achieve a 15 MHz cut-off frequency with sharp roll-off, minimal gain error, and reduced pass-band ripple. To enhance stability and common-mode rejection, the OTA integrates both common-mode feed-forward (CMFF) and a modified common-mode feedback (CMFB) circuit. Post-layout simulations demonstrate a cut-off frequency of 15 MHz, a phase margin of 79°, and improved linearity compared to conventional Gm-C designs. These results confirm that the enhanced OTA architecture offers superior tuning capability, robust common-mode suppression, and reliable high-frequency performance. The contribution of this work lies in providing a compact, high-performance solution for analog front-end signal conditioning, representing a significant improvement over existing CMOS Gm-C filter implementations.

1. Introduction

Gm-C topology filters are popularly employed for a wide range of applications, including Microsensor readout, body area network communication, and biomedical signal processing. They can be implemented using either the conventional operational amplifiers or special purpose Operational Transconductance Amplifier (OTA), depending on the specific requirements of the application. Transconductance-based filters enhance linearity and stability of the filters hence are much preferred. Various methods and techniques have been implemented recently, which include maintaining constant gate-source voltages, source degeneration, nonlinearity minimization, employing floating-gate transistors and feedback amplifiers. However, there is an increasing demand to enhance the gain and stability for application such as Microsensor readout application.

In recent years, there were several techniques proposed to enhance the gain of OTA with minimal power consumption that caters for portable Microsensor applications. Few notable techniques are pseudo-differential amplifiers, current-mode circuits, bulk driven, and floating gate transistor technique. Alternative technique to enhance phase margin, which eventually yields better linearity and stability without compromising gain and bandwidth is essential. Such OTAs when implemented to design the Gm-C filter, desired cut-off frequency in the range of MHz is achievable with better linearity and stability. This paper introduces an OTA design with feedback network that can yield a cut-off frequency of 15 MHz when employed in the Gm-C filter stage. Section 2 of this paper describes the design techniques of OTA, whereas in section 3, Gm-C topology and the design methodology are discussed. Section 4 deals with the simulation result analysis of both the designs. Finally, the work is concluded with a note to future work is presented.

2. Design of Enhanced Tuned OTA

The inverter based tuned OTA proposed in [1] is suitable to operate at high frequencies, which do not fulfil the requirement of low frequency applications, especially the interface electronics circuits utilized for readout purposes. Further, it is observed to have poor stability in the specific frequency of interest. Other existing tuned OTAs found to have common mode voltage as high as half the supply voltage to keep all the transistor in saturation region. On the other hand, in [2] and [3] the bulk voltages of the transistors have been varied complimentarily for PMOS and NMOS transistors, due to these variations the threshold voltages of transistors also varies and transconductance are varied abruptly, yielding poor performance.

In this work, the structures and arrangement of devices are built as shown in Fig. 2. For last half a decade, there are no significant filter design proposed targeting low frequency interface electronics application. In this work, the enhanced tuned OTA has been designed for ultra-low frequency to overcome the drawbacks of the existing tuned OTA which do not cater for such frequency range operation of interface electronics. The enhanced tuned OTA shown in Fig. 1, operates as pseudo-differential circuit that comprises of CMFF, CMFB, and Input inverter. Transconductance of the amplifier depends on the transistors M1-M2 and M3-M4. Pseudo-differential structure CMOS inverters are employed due to their good linearity. There are no parasitic zeroes and poles, because of their single stage structure and well matched for low voltage scenarios. Transistor M5-M6 and M9-M10 are cross-coupled at output to optimize the differential gain and produce negative resistance to increase the impedance of output side. Common mode voltage is intentionally set at half of the supply voltage and all the transistor in saturation region.

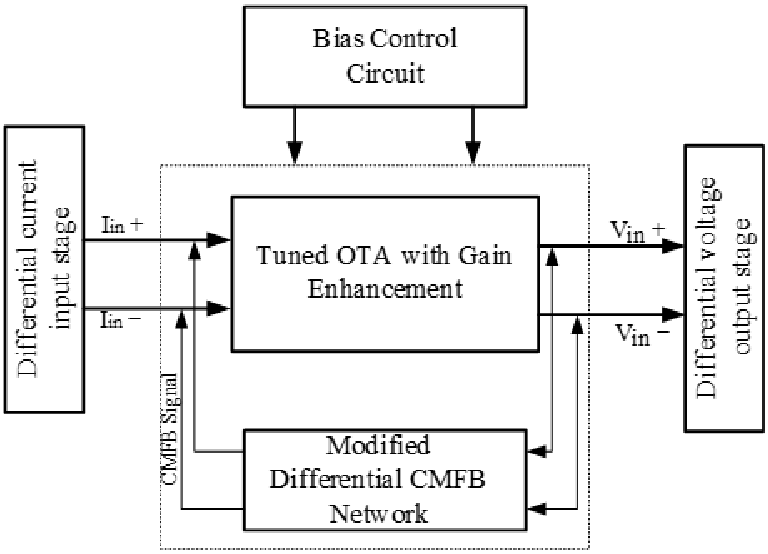

Fig. 1 *Block diagram of tuned OTA with modified differential CMFB*

Fig. 1 illustrates the block diagram of the proposed tuned operational transconductance amplifier (OTA) with gain enhancement and modified differential common-mode feedback (CMFB). The architecture consists of a differential current input stage that converts the input signals I_{in+} and I_{in-} into corresponding differential voltages, which are processed by the tuned OTA core. The OTA incorporates gain enhancement techniques to achieve high differential gain while maintaining wide bandwidth. A bias control circuit provides stable biasing to the OTA core, ensuring robust operation across process, voltage, and temperature variations. The modified differential CMFB network senses the output common-mode voltage and generates a corrective feedback signal to regulate the common-mode level, thereby stabilizing internal bias points and improving linearity under large differential signal swings. The regulated outputs V_{out+} and V_{out-} are delivered through a differential voltage output stage. This combined CMFB and gain-enhanced OTA architecture enables improved common-mode regulation, enhanced stability, and superior linearity, making it well suited for high-performance Gm–C filter applications.

Common mode feed-forward (CMFF) and Common mode feedback (CMFB) circuits were implemented in tuned OTA to reduce the common mode gain, thereby increasing common mode rejection ratio [2]. To stabilize the enhanced tuned OTA, the feed-forward network has been modified with CMOS active resistors in series as shown in Fig. 2. Due to this modified CMFF, a 24 dB of common mode gain is achieved, which is less than the existing tuned OTA. Open loop gain is increased by 5 dB compared with existing tuned OTA. Much care in the design has been considered not to exceed a phase margin of above 80°, which can lead to potential overshoot. This has been the case in the existing tuned OTA with a phase margin of 87°. The phase margin of enhanced tuned OTA is 79°, which is 8° less than the existing tuned OTA that eliminated the concern of potential overshooting.

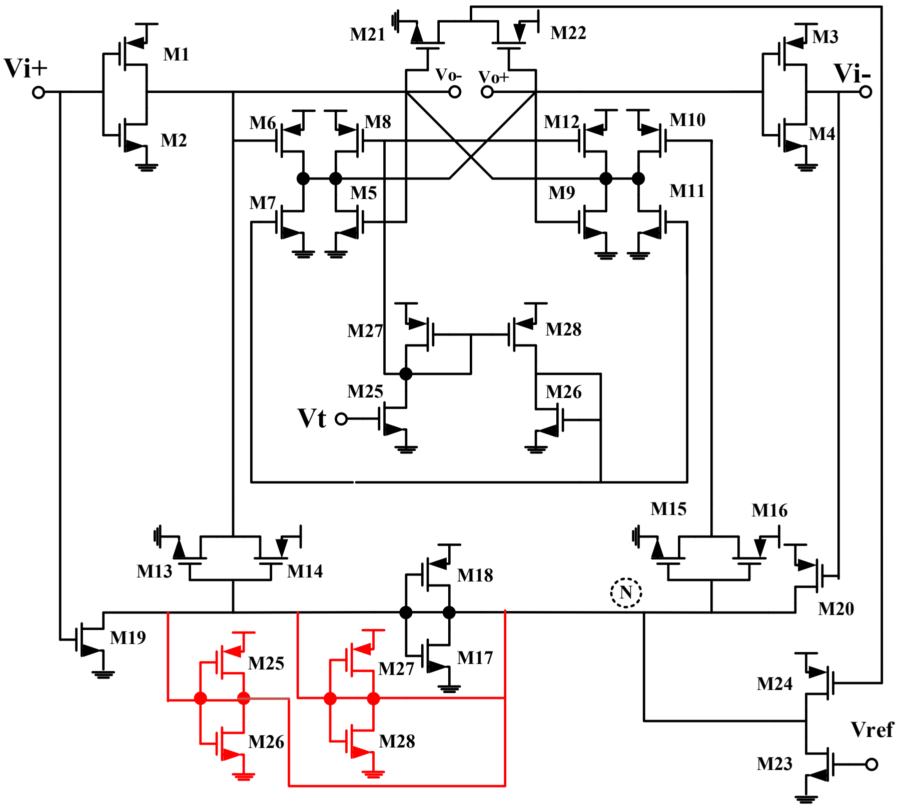

Fig. 2 *Enhanced tuned OTA with modified differential CMFB circuit*

The differential and common mode resistance produced by M5-M12 are as in (1) & (2):

$$R_{DIFF} = r_{05}||r_{07}||(\frac{1}{-gm_5}) \tag{1}$$

$$R_{CM} = \frac{1}{2}\left[r_{05}||r_{07}||(\frac{1}{gm_5})\right] \tag{2}$$

The optimized aspect ratios of the transistors designed in the tuned OTA to achieve the desired performances are listed in Table 1. The designed enhanced tuned OTA is satisfactory to be employed in the Gm-C filter design. The methodology involved in the design of Gm-C filter is discussed in the next section.

Table 1 *Transistors aspect ratios*

Transistor	*Dimensions in nm*	
	W_N/L_N	W_P/L_P
M5, M7, M9, M11	130/200	-
M6, M8, M10, M12	-	365/100
Rest of the transistors	600/120	1180/100

3. Gm-C Filter Design

Gm-C filters are a class of continuous-time analog filters that utilize operational transconductance amplifiers (OTAs) and capacitors to perform filtering functions. These filters are particularly well-suited for integration in modern CMOS technologies due to their compatibility with voltage-mode circuits and their ability to achieve tunable frequency characteristics by varying the transconductance (Gm) of the OTA. Unlike active-RC filters, Gm-C filters eliminate the need for precision resistors, making them more area- and power-efficient. Their wide tuning range, high-frequency operation, and ease of integration make Gm-C filters highly attractive for applications in wireless communication, data converters, biomedical signal processing, and low-voltage analog signal conditioning. However, challenges such as linearity, noise, and process variation sensitivity must be carefully addressed in practical implementations. Gm-C filters have been found popularly employed in read out electronics due to its low gain error and better roll off. Most Gm-C stages include multiple OTA stages as Gm network and capacitors to achieve the desired responses. Designing Gm-C filters involves careful consideration of the transconductance element's linearity, frequency response, and biasing stability. The fundamental building block, the operational transconductance amplifier (OTA), converts input voltage into output current, and its transconductance value directly controls the filter's cut-off frequency. Since the frequency characteristics depend on the ratio of Gm to capacitance (fc $\propto$ Gm/C), tuning can be efficiently achieved by adjusting the OTA's bias current. However, practical design must account for non-idealities such as limited output swing, parasitic capacitance, and distortion at high signal levels. Advanced Gm-C filter architectures may employ techniques like source degeneration, linearization circuits, or differential topologies to enhance performance, especially in low-voltage or high-speed environments. Balancing these design trade-offs is crucial for achieving robust, scalable analog filtering solutions in modern integrated systems.

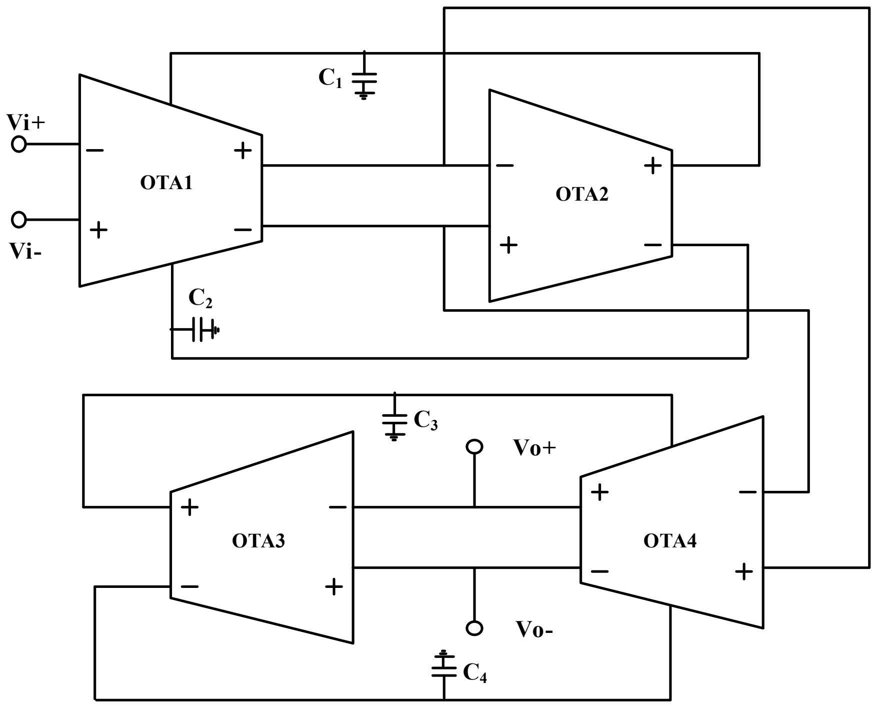

Fig. 3 *Block diagram of fourth order Gm-C low pass filter*

Over the decade, such filter designs have been extensively researched for its employment in various applications. Hu et al. [3] presented a 4th order Gm-C low-pass filter with a wide tuning range targeting high-frequency applications, implemented in CMOS technology with an emphasis on frequency agility and compact integration. Similarly, Wang et al. [4] introduced a low-noise, widely tunable Gm-C filter with on-chip frequency calibration, enhancing reliability and precision over a broad frequency range, which is crucial for RF and mixed-signal systems. Namdari et al. [5] developed a 0.5 V, ultra-low-power Gm-C filter for bio-signal processing, showcasing inverter-based topology to enable all-filtering responses while consuming only 32 nW suitable for implantable or wearable devices. Oliveira et al. [6] designed a digitally tunable Gm-C filter aimed at multi-standard receivers, demonstrating high configurability and frequency agility while using a 180 nm CMOS process. Akbarian et al. [7] proposed a modified low-voltage Gm-C architecture utilizing impedance boosting through body-driven techniques to enhance gain and linearity while maintaining low power operation, addressing common trade-offs in compact analog designs.

Int. Journal of Integrated Engineering Vol. 17 No. 6 (2025) p. 59-71

Further addressing tuning challenges, Jha et al. [8] introduced a mixed-mode automatic frequency tuning technique for bio potential amplifiers, which can be effectively integrated with Gm-C filters to ensure consistent frequency behaviour under varying conditions. Finally, Mincey et al. [9] presented a low-power 6^{th} order Gm-C filter employing current-reuse differential difference amplifiers, which achieved excellent power efficiency and linearity, making it suitable for high-speed signal conditioning in communication systems. These works highlight diverse innovations in Gm-C filter design, ranging from biomedical to RF applications [10], emphasizing low-voltage operation, tunability, compactness, and integration with calibration or adaptive features.
The block diagram featured in Fig. 3 illustrates a single stage linear phase tunable Gm-C filter, which has been sequentially connected to form fourth order filter. Given arrangement of transconductance in this circuit, there is no need for dedicated common-mode voltage detector within the CMFB circuit. This is because the output common-mode voltage value is extracted from CMFF circuits of the subsequent filter stage. Consequently, by consolidating the CMFB and CMFF circuits, two transistors can be eliminated in each filter stage, four CMFB circuits are necessary to maintain the stability of the output common-mode level.

For a Gm-C filter, the proposed 4^{th} order cut-off frequency depends on OTAs 3 and 4 of Fig 3., its frequency with transconductance and capacitor sizing are as follows [17]:

$$f_c = \frac{1}{2\pi}\sqrt{\frac{G_{m3}G_{m4}}{C_3C_4}} \quad (2)$$

When the target cut-off frequency is 15 MHz, then the required transconductance can be arrived through the following relationship: [17]

$$G_m = 2\pi f_c C \quad (3)$$

Where, C is calculated as C_3 cascaded with C_4, i.e., $C = C_3.C_4$, by fixing the frequency and choosing the capacitance the transconductance can be calculated.

The gm of each CMOS devices calculated from the expression under strong inversion condition is [11],

$$g_m = \sqrt{\mu_n C_{ox}\frac{W}{L}I_D} \quad (4)$$

For OTA-C filters, phase margin is governed by OTA internal poles ω_p (mainly due to load capacitances C_L and parasitics), given by [11];

$$PM = 90^o - \left(\frac{\omega_{UGF}}{\omega_p}\right) \quad (5)$$

Whereω_{UGF}, can be given by;

$$\omega_{UGF} = \frac{G_m}{C_L}\sqrt{\mu_n C_{ox}\frac{W}{L}I_D} \quad (6)$$

The upper portion of the proposed filter comprises OTA1 and OTA2 in conjunction with capacitors C_1 and C_2**,** forming the first second-order gm-C section**.** OTA1 converts the applied differential input signal (I_{in}+, I_{in}−) into a proportional transconductance voltage, while OTA2 provides the necessary feedback to realize the intended pole - zero configuration. Capacitors C_1 and C_2 function as continuous-time integrating elements and store the state variables of the system. In combination with the transconductances of OTA1 and OTA2, they generate the first complex-conjugate pole pair of the overall transfer function. The pole frequency and quality factor of this section are primarily determined by the transconductance-to-capacitance ratios, g_{m1}/C_1 and g_{m2}/C_2, respectively. Similarly, the lower portion of the circuit forms the second second-order section, composed of OTA3 and OTA4 and capacitors C_3 and C_4**.** The output of the first section drives this stage, resulting in a cascade configuration. Capacitors C_3 and C_4 perform the same integrative function as C_1 and C_2 but correspond to the third and fourth poles of the filter. The fully differential structure ensures symmetric signal processing, yielding complementary outputs V_{out}+ and V_{out}−. This section completes the realization of the fourth-order transfer characteristic. In fully differential g_m-C filters the CMFB loop must enforce the desired common-mode voltage without injecting significant disturbance into the differential signal loops. If the CMFB is too slow or poorly decoupled, CM error modulates the OTA tail currents and shifts effective g_m, moving poles and degrading filter response [12].

The proposed modified differential CMFB topologies increase the CM loop bandwidth while preserving phase margin which the CM loop tracks output CM variations faster and reduces CM-to-differential coupling. That yields more stable pole placement across signal conditions and less low-frequency distortion. Target CMFB bandwidth ≈ (0.5–1)× differential pole frequency (or higher) and ensure CMFB compensation does not introduce right-half-plane zeros that interact with the differential loop. For applications involving large differential signal swings, feed-forward common-mode sensing techniques are preferred to ensure robust common-mode regulation. By minimizing common-mode error and maintaining stable biasing conditions, modified common-mode feedback (CMFB) OTA architectures effectively reduce harmonic distortion and intermodulation distortion (IMD), particularly under large-signal excitation.

Prior studies on CMFB-enhanced OTA designs consistently report improved THD and IMD performance, attributed to the mitigation of output swing-dependent bias variations through enhanced common-mode control. In Gm-C filters, the pole frequency is primarily determined by the relation $\omega_p \approx g_m/C$, and CMFB influences pole accuracy only indirectly through its impact on transconductance stability. Variations in common-mode voltage can alter the transistor overdrive voltage, thereby affecting gm. Consequently, improved common-mode regulation leads to a more stable transconductance, resulting in tighter and more accurate pole placement across process, voltage, temperature (PVT) variations and input signal swing [13].

Improved common-mode (CM) control enables larger usable differential signal swings by preventing device stack saturation and mitigating undesirable CM voltage drift. Modified common-mode feedback (CMFB) architectures that actively compensate for swing-dependent CM variations consequently enhance the achievable dynamic range, commonly quantified in terms of output signal-to-noise ratio (SNR) or dynamic range (DR) at the filter output. These benefits are particularly pronounced in low-supply-voltage designs operating below 1.2 V, where limited voltage headroom increases susceptibility to bias instability. However, such modified CMFB networks generally exhibit higher design complexity compared to conventional resistor- or capacitor-based CMFB implementations, often requiring additional circuitry to achieve effective CM regulation. Advanced common-mode feedback (CMFB) implementations may require additional circuit elements, such as auxiliary amplifiers, switches, or sensing detectors, which inevitably lead to increased silicon area and marginal additional power consumption [14]. Nevertheless, in high-performance filter applications, these overheads are often justified by the resulting improvements in linearity, stability, and reduced sensitivity to tuning inaccuracies. From an analytical standpoint, the CMFB loop introduces a corrective common-mode control term that stabilizes internal bias conditions and indirectly influences the small-signal differential transconductance.

4. Results and Simulation Analysis

The designed enhanced tuned OTA in 90 nm CMOS technology is analysed for its performance to verify the suitability of utilization in Gm-C filter application. The proposed operational transconductance amplifier (OTA) exhibits a well-controlled and tunable frequency response, achieving an open-loop differential gain of 39 dB, as illustrated in Fig. 4. The gain characteristic demonstrates stable amplification across the frequency range of interest, confirming the effectiveness of the tuning and gain-enhancement mechanisms employed in the OTA architecture. In addition, the common-mode gain of the proposed OTA remains extremely low over the same frequency range, as shown in Fig. 5. The minimal variation in common-mode gain indicates effective common-mode suppression, which can be attributed to the modified common-mode feedback (CMFB) network and robust bias control. This strong rejection of common-mode signals ensures improved linearity, enhanced stability, and reduced susceptibility to noise and interference, thereby validating the suitability of the proposed OTA for high-performance Gm–C filter applications.

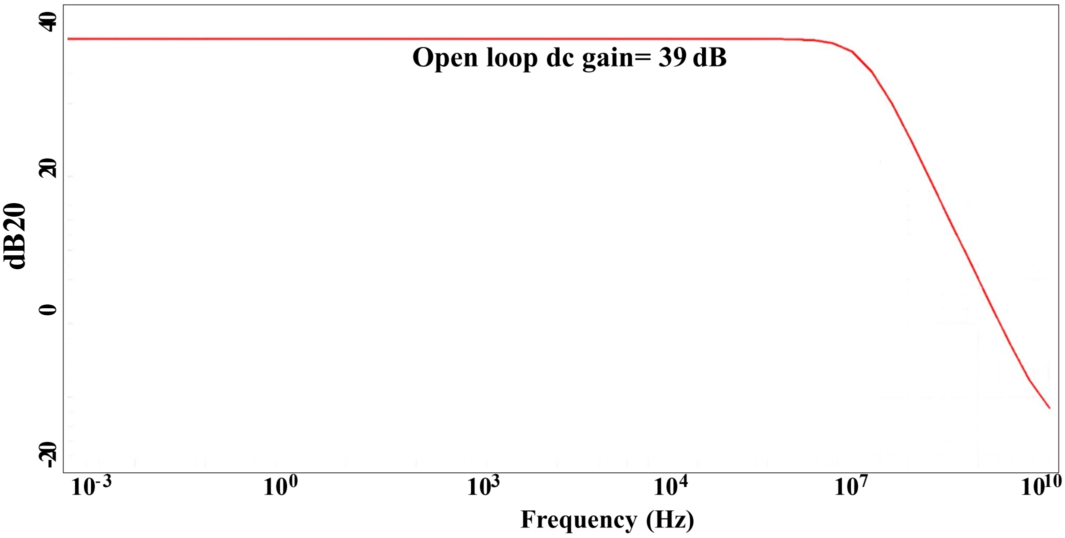

Fig. 4 *Open loop gain of enhanced tuned OTA*

The low common-mode gain achieved by the proposed OTA results in a high common-mode rejection ratio (CMRR), making it particularly suitable for low-frequency active filter applications where common-mode disturbances can significantly degrade performance. The large-signal linearity of the enhanced OTA is further characterized by its 1 dB compression point, measured at −2.86026 dB, as illustrated in Fig. 6, which defines the maximum input level for linear operation. In addition, intermodulation distortion (IMD) performance is evaluated using a two-tone test to determine the third-order intercept point (IP3), providing insight into the OTA's nonlinear behavior under multi-tone excitation. The corresponding IMD results are also presented in Fig. 6. Furthermore, the total harmonic distortion (THD) is analyzed over a frequency range up to 1 GHz, with the results shown in Fig. 6, demonstrating suppressed harmonic components and improved linearity. Collectively, these results confirm that the proposed OTA exhibits strong linearity and distortion performance, reinforcing its suitability for high-performance Gm–C filter implementations.

When compared to existing works, such as [15] and [16], which employ linearization techniques to enhance OTA linearity, the presented OTA demonstrates competitive distortion performance without excessive complexity in circuit architecture.

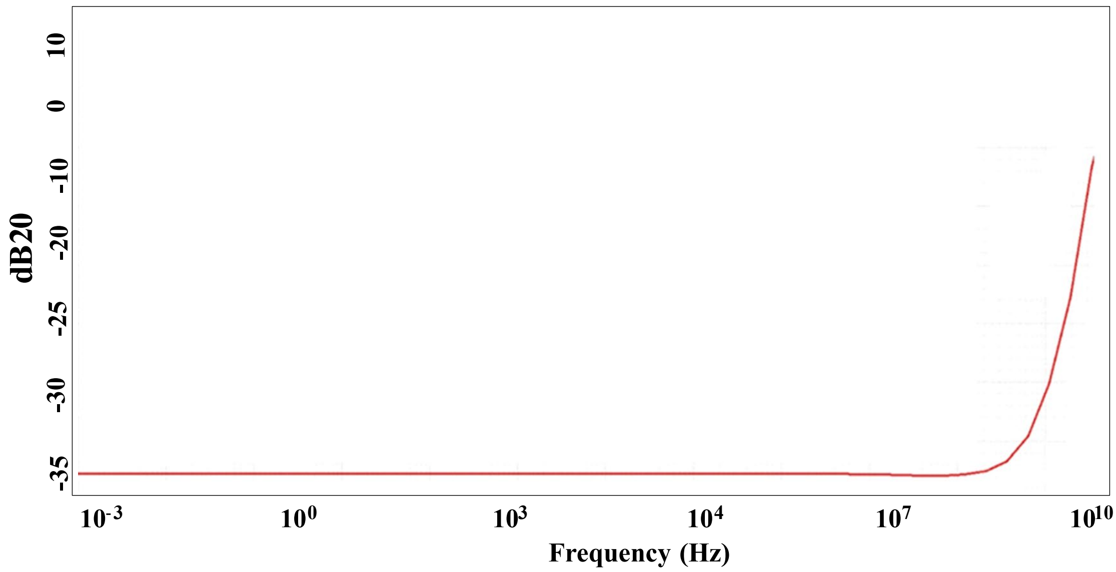

Fig. 5 *Common mode gain of enhanced tuned OTA*

Unlike the designs in [16] and [17], which focus on GHz-range cut-offs using complex automatic tuning schemes, our approach achieves a lower cut-off frequency of 15 MHz, more suitable for narrowband applications, while maintaining low noise and THD.

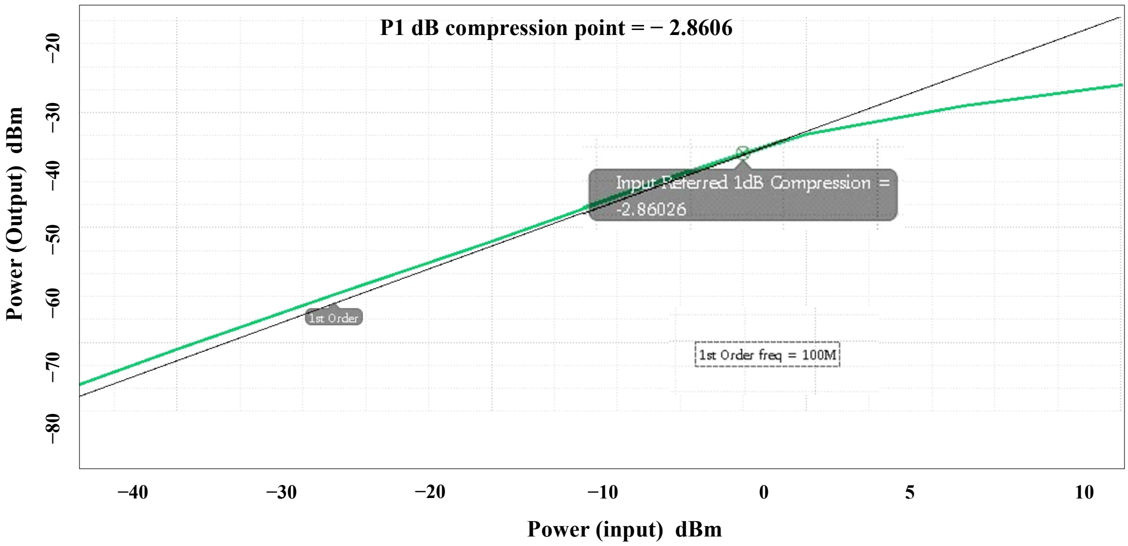

Fig. 6 *1 dB compression point of enhanced OTA*

Furthermore, compared to the adaptive biasing method in [18], our OTA offers comparable noise performance with a simpler implementation. The overall results validate the effectiveness of the proposed design in achieving high linearity and low noise in a tunable OTA-filter configuration.

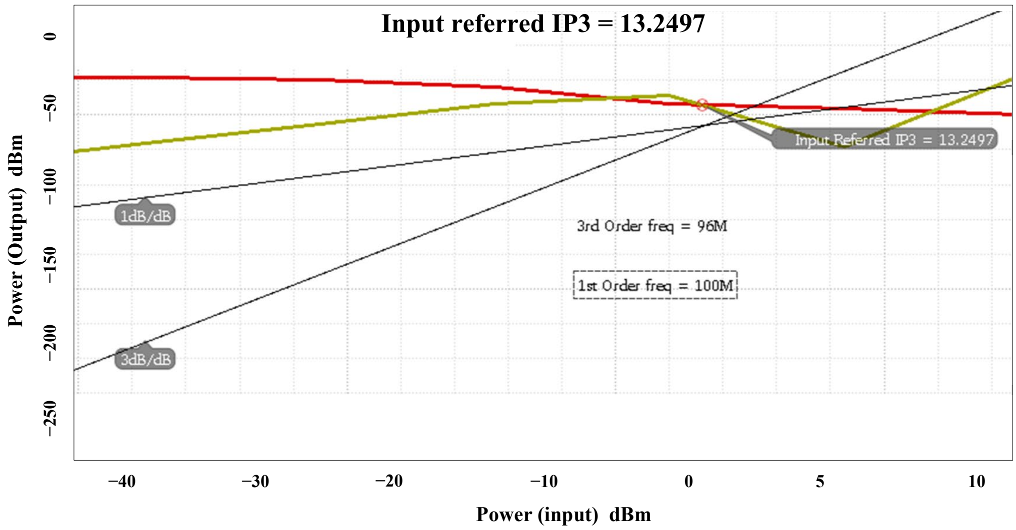

Fig. 7 *Simulation of IP3 of OTA with modified CMFB*

The simulated third-order intermodulation performance (IP3) of the OTA improved after implementing the modified common-mode feedback (CMFB) network: two-tone transient simulations from Fig. 7, show that the IM3 products are reduced and the extrapolated OIP3 moves to a higher output power intercept compared with the baseline OTA. This improvement is attributable to the modified CMFB's tighter regulation of the output common mode voltage under large differential swings, which preserves device operating points and reduces gm modulation and device mismatch induced even or odd nonlinearities. Otherwise, by keeping the output nodes closer to their optimal bias the OTA stays in a more linear region for larger signals. Additional mechanisms include improved symmetry of the differential pair which used to reduce common mode excursions that otherwise create even order distortion and any intentional local feedback inside the CMFB that linearizes the output node impedance. The simulation also revealed that IP3 value 13.2497 which obtained through the modified CMFB and

Int. Journal of Integrated Engineering Vol. 17 No. 6 (2025) p. 59-71

it introduce an extra low-frequency pole and loop dynamics that must be stabilized and may result in slightly increase power or noise depending on how the CMFB is biased as described a common trade-off.

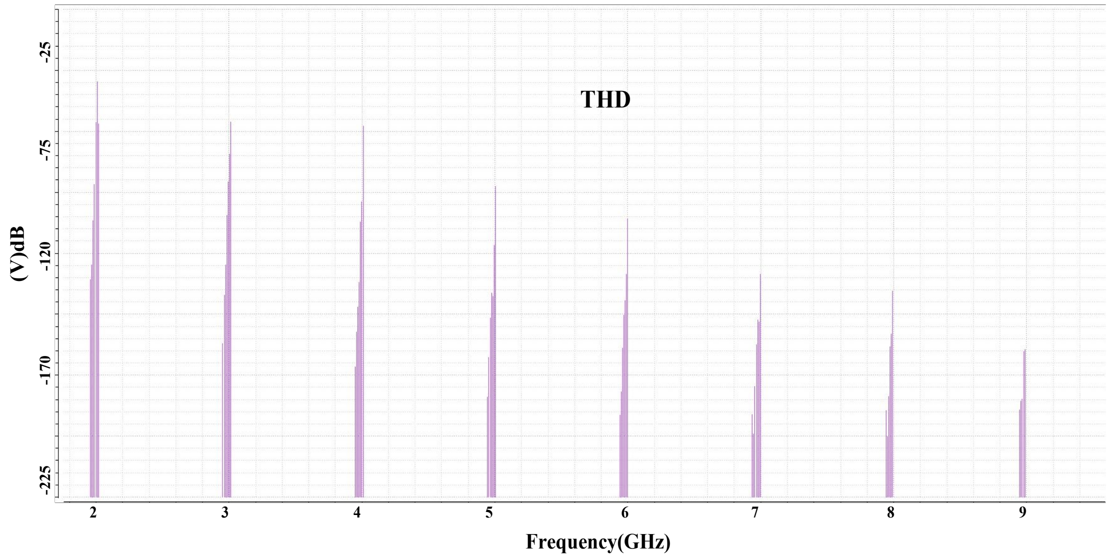

Fig. 8 *THD simulation of OTA with modified CMFB*

As shown in Fig. 7, the spectral components appearing at 2, 3, 4, … GHz correspond to the harmonic frequencies of the fundamental signal. The highest-magnitude spectral peak represents the fundamental frequency component, whereas the lower-magnitude peaks observed at integer multiples of the fundamental frequency correspond to higher-order harmonics. The presence of these harmonic components indicates non-linear characteristics in the system response.

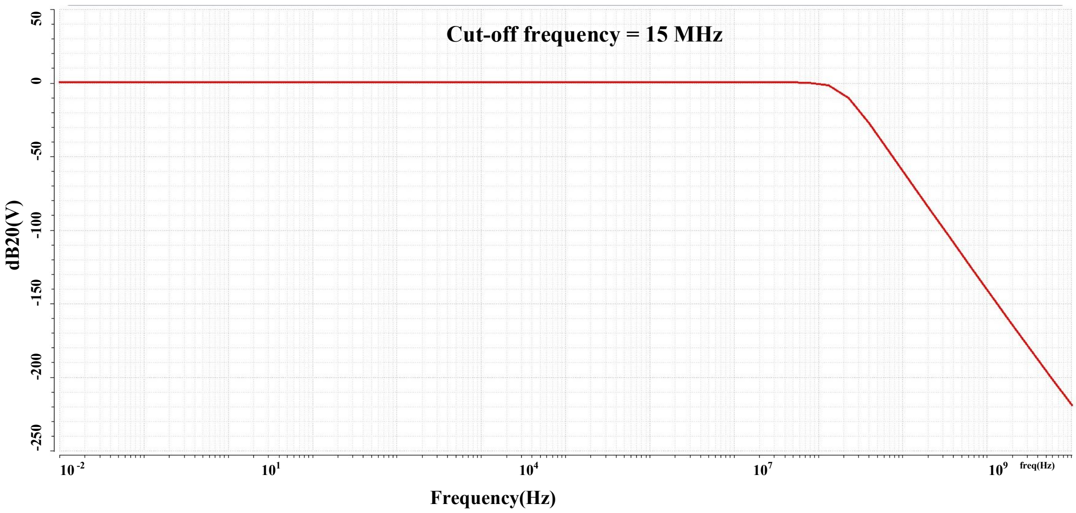

Fig. 9 *Simulated AC magnitude response of the proposed OTA-based low-pass filter with a −3 dB cut-off frequency of 15 MHz*

To evaluate the performance of the proposed Gm-C low-pass filter built using the designed enhanced tuned OTA, a comparative analysis has been conducted against selected state-of-the-art designs reported in the literature. The frequency response of a 4th-order CMOS Gm–C filter implemented with operational transconductance amplifiers (OTAs) is governed by the interaction between the OTA transconductances and the integrating capacitors that form the filter's biquads sections. In such architectures, each OTA performs a voltage-to-current conversion whose small-signal transconductance gm determines the effective conductive weight within the continuous-time filter, while the capacitors establish the dynamic storage necessary to realize the complex conjugate pole pairs of the 4th-order transfer function. Because the pole frequencies scale proportionally with the ratio gm/C, digitally controlled biasing or current-scaling techniques allow the filter to achieve a very wide tuning span from low audio-range frequencies around 500 Hz up to high-frequency operation approaching 15 MHz shown in Fig. 9.

Table 2 summarizes key performance metrics, implementation technologies, and design characteristics of the proposed work alongside those in references [3], [1], and [19].

Table 2 *Comparing the performances of filters*

Design parameters	This work	[9]	[15]	[12]
Technology	90 nm CMOS	90 nm CMOS	28 nm SOI CMOS	180 nm CMOS
Order of the filter	4	4	3	4
Filter type	LPF Gm-C	LPF Gm-C	LPF Gm-C	LPF Gm-C
fc	15 MHz	1 GHz	459 MHz	1 GHz
Supply voltage	1 V	1 V	1 V	1.5 V
Automatic tuning	Yes	Yes	Yes	Yes
Gain of the OTA	39 dB	34 dB	-	-
Phase margin	79°	87°	-	-
Common mode gain of the OTA	-24 dB	-26 dB	-	-

At the lower end of this range, the frequency response is primarily limited by leakage effects, finite OTA output resistance, and noise constraints, all of which tend to reduce the achievable Q-factor and therefore require larger capacitor values or enhanced linearity techniques to maintain accurate pole placement. Conversely, at the upper end of the tuning range, the response becomes sensitive to high-frequency non-idealities such as parasitic capacitances, finite OTA gain-bandwidth product, and transistor Cgd feedthrough, which introduce additional poles and zeros that can distort the ideal response and reduce stopband attenuation. When implemented as two cascaded second-order Gm-C biquads, the 4th-order filter can be synthesized for Butterworth, Chebyshev, or custom amplitude characteristics by appropriate selection of Q-enhancing feedback coefficients and relative transconductance scaling, enabling precise control of magnitude flatness, transition-band steepness, and dynamic range. As a result, shown in Fig.8, with careful device sizing and parasitic-aware CMOS tuning circuitry, a 4th-order OTA-based Gm–C filter can preserve stable, low-distortion performance and accurate pole–zero placement across its entire 500 Hz–15 MHz operating range, making it highly suitable for wideband analog front-ends, programmable bio signal interfaces, and mixed-signal system-on-chip applications.

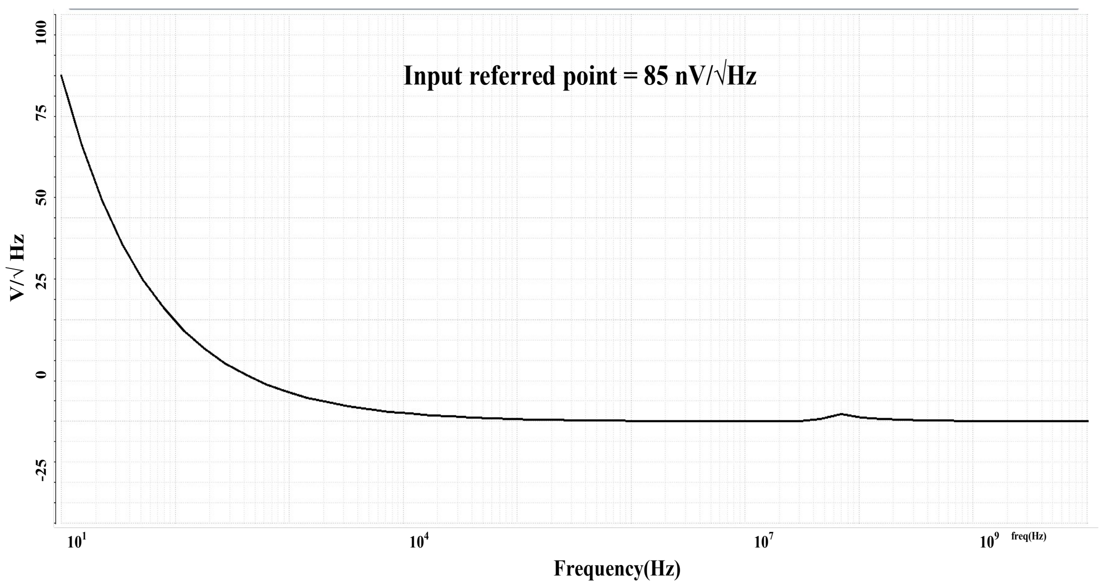

Fig. 10 *Simulated input-referred noise spectrum of the proposed OTA-based filter*

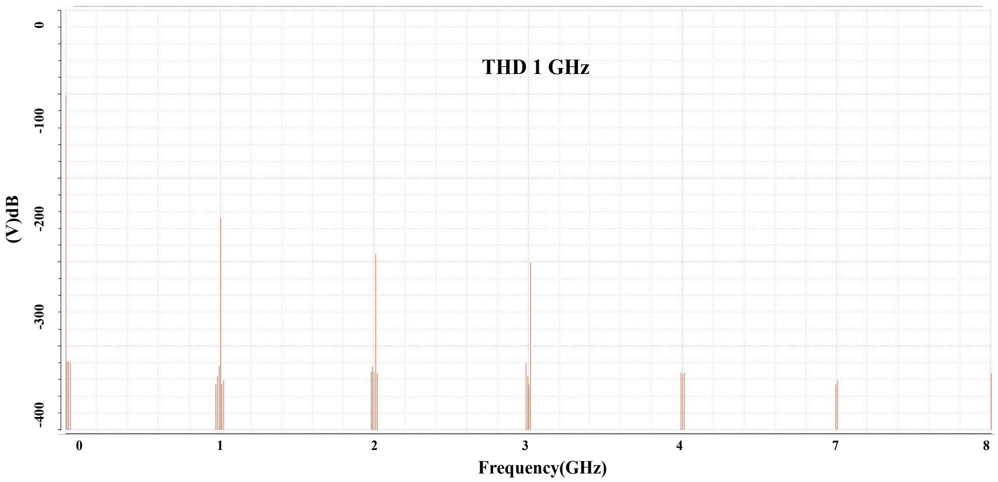

Fig. 11 *THD simulation results of the proposed OTA-based filter operating at 1 GHz*

The frequency response of the implemented OTA-based filter is illustrated in Fig. 9. The plot demonstrates a well-defined low-pass characteristic with a sharp roll-off occurring at a cut-off frequency of 15 MHz. The flat passband response indicates stable gain behavior within the operating bandwidth, while the rapid attenuation beyond the cut-off frequency confirms the effective suppression of high-frequency components. These results validate the accuracy of the proposed filter design and its suitability for high-frequency signal conditioning applications.

The input-referred noise performance of the proposed filter is depicted in Fig. 10. The simulation results indicate an input-referred noise spectral density of approximately 85 nV/√Hz across the mid-band region. The noise spectrum exhibits higher noise levels at low frequencies due to flicker noise, followed by a relatively flat noise floor at higher frequencies. This low input-referred noise demonstrates the effectiveness of the OTA architecture in achieving noise-efficient operation, which is critical for precision analog signal processing. The linearity performance of the filter is evaluated through total harmonic distortion (THD) analysis, as shown in Fig. 11 for a 1 GHz input signal. The harmonic spectrum reveals a dominant fundamental component with significantly attenuated higher-order harmonics, indicating low distortion operation. The observed THD performance confirms that the proposed filter maintains adequate linearity within the intended operating range, making it suitable for high-frequency and low-distortion applications.

Table 2 explores the performance comparison with prior Gm-C filter designs. The proposed filter is designed using a 90nm CMOS process, similar to the implementation in [3], while [19] leverages a more advanced 28 nm SOI CMOS process, and [5] employs a relatively older 180 nm CMOS node. All four designs adopt the Gm-C low-pass filter topology, though they vary in design complexity and target specifications.

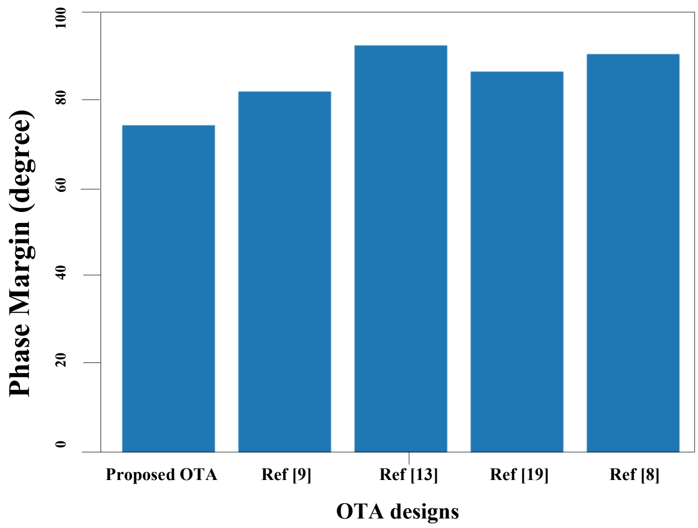

Fig. 12 *Phase margin comparison of the proposed OTA with existing OTA designs*

The proposed filter achieves a 4th order configuration, consistent with [3] and [5], whereas [8] utilizes a 3rd-order architecture. A notable difference is observed in the cut-off frequency (f_c), where the proposed design operates at 15 MHz. This is significantly lower than the 1 GHz reported in [3] and [5], and the 459 MHz in [8]. The reduced bandwidth in the proposed design is optimized for applications prioritizing low-frequency operation and potentially improved power efficiency and noise performance.

All OTA designs operate with automatic tuning capability, enabling adaptability to process, voltage, and temperature (PVT) variations. The proposed design, [3], and [8] function at a low supply voltage of 1 V, enhancing their suitability for low-power applications, whereas [5] requires a higher voltage of 1.5 V. In terms of transconductance amplifier (OTA) performance, the proposed design exhibits a gain of 39 dB, which surpasses the 34 dB reported in [3]. Gain values for [17] and [11] are not disclosed. The phase margin of the proposed design is 79°, slightly lower than the 87° achieved in [9], yet still indicative of a stable system response shown in Fig.12.

The common-mode gain of the OTA in the proposed work is measured at -24 dB, compared to -26 dB in [3]. No corresponding data are available in [15] and [18]. Finally, the input-referred noise of the proposed filter is 85 nV/√Hz, which is marginally higher than the 80 nV/√Hz reported in [19], while [20] does not specify this metric. Overall, the proposed Gm-C filter demonstrates competitive performance with favourable characteristics in OTA gain, power supply requirements, and automatic tuning, while targeting lower-frequency applications with strong stability and acceptable noise levels.

Gm-C filter design has significantly improved performance across various applications, especially in signal conditioning and low-power analog processing.

5. Conclusion

The enhanced tunable operational transconductance amplifier (OTA) based Gm-C low pass filter is implemented with GPDK 90 nm technology. This enhanced tuned OTA integrated with CMFF and CMFB circuits to achieve better performance in differential DC gain and unity gain frequency of 39 dB and 10 GHz respectively. Furthermore, the proposed design exhibits a phase margin of 79°, confirming robust closed-loop stability while maintaining high-speed operation. The cut-off frequency of the LPF is obtained as 15 MHz and it is suitable for signal conditioning in analog interface electronics. Further this work may lead to pave way to design high performance Gm-C filter for any low frequency interface circuits.

Acknowledgement

I would like to express my sincere gratitude to my research supervisor Dr. Ananiah Durai S, at Centre for Nano-Electronics and VLSI Design (CNVD), Vellore Institute of Technology, Chennai, for their invaluable guidance, continuous encouragement, and insightful technical discussions throughout of this research work on OTA-based 4th-order Gm–C filter design and linearity enhancement.

Conflict of Interest

Authors declare that there is no conflict of interests regarding the publication of the paper.

Author Contribution

The authors confirm contribution to the paper as follows: ***study conception and design:*** *Author 1, Author 2;* ***data collection:*** *Author 3;* ***analysis and interpretation of results:*** *Author 1, Author 3;* ***draft manuscript preparation:*** *Author 2. All authors reviewed the results and approved the final version of the manuscript.*

References

[1] Abdulaziz, M., Ahmad, W., Tormanen, M., & Sjoland, " A linearization technique for differential OTAs", IEEE Transactions on Circuits and Systems II, 64(9), 1002–1006, December 2017. DOI: 10.2174/2352096512666191019130214

[2] Abdolmaleki, M., Dousti, M., & Tavakoli, M. B, "Design and simulation ofourth order low-pass Gm-C filter with novel auto-tuning circuit in 90nm CMOS", Analog Integrated Circuits and Signal Processing, 107(1), May 2019. https://doi.org/10.1016/j.mejo.2017.06.008

[3] Hu, Jin & Hei, Huage & Liu, Qingbo & Liu, Guancheng. (2009). CMOS 4(th)-order Gm-c Low-Pass Filter with Wide tuning Range in High Frequency. 10.1109/ASICON.2009.5351462. DOI:10.1109/ASICON.2009.5351462.

[4] Y Wang, J Liu, N Yan, H Min. A low-noise widely tunable Gm-C filter with frequency calibration[J]. J. Semicond., 2016, 37(9): 095002. doi: 10.1088/1674-4926/37/9/095002.

[5] Namdari, A.; Aiello, O.; Caviglia, D.D. A 0.5 V, 32 nW Compact Inverter-Based All-Filtering Response Modes Gm-C Filter for Bio-Signal Processing. J. Low Power Electron. Appl. 2024, 14, 40. https://doi.org/10.3390/jlpea14030040

[6] Oliveira, M.S.; Carvalho, M.B.S.; Müller, C.; Compassi-Severo, L.; de Aguirre, P.C.C.; Girardi, A.G. Design and Characterization of a Digitally Tunable Gm-C Filter for Multi-Standard Receivers. Electronics 2024, 13, 2866. https://doi.org/10.3390/electronics13142866

[7] Seyed Mohammad Fahmideh Akbarian, Reza Lotfi, and Mohammad Maymandi-Nejad,"Low-voltage low-power Gm-C filters: a modified configuration for improving performance", Analog Integr. Circuits Signal Process. 74, 1 (January 2013), 297–302. https://doi.org/10.1007/s10470-012-9973-x

[8] Pankaj Kumar Jha, Pravanjan Patra, K. R. Jairaj Naik, Ashok Singh, and Ashudeb Dutta, "A mixed-mode on-chip automatic frequency tuning technique for biopotential amplifiers", Analog Integr. Circuits Signal Process. 122, 1 (Jan 2025). https://doi.org/10.1007/s10470-024-02294-9.

[9] J. S. Mincey, C. Briseno-Vidrios, J. Silva-Martinez and C. T. Rodenbeck, "Low-Power Gm−C Filter Employing Current-Reuse Differential Difference Amplifiers," in IEEE Transactions on Circuits and Systems II: Express Briefs, vol. 64, no. 6, pp. 635-639, June 2017, doi: 10.1109/TCSII.2016.2599027.

[10] S. Ahmed Aamir and J. Jacob Wikner, "A 1.2-V pseudo-differential OTA with common-mode feedforward in 65-NM CMOS," 2010 17th IEEE International Conference on Electronics, Circuits and Systems, Athens, Greece, 2010, pp. 29-32, doi: 10.1109/ICECS.2010.5724446.

[11] J B Yogeshwar, Naushad Manzoor Laskar, Alan Samuel, Alwin Solomon, Vikas Vijayvargiya, "Design and analysis of low noise, low power OTA considering design trade-offs for biomedical applications", Results in Engineering, Volume 26, 2025, 105103, ISSN 2590-1230, https://doi.org/10.1016/j.rineng.2025.105103.

[12] Ali Namdari, Mehdi Dolatshahi, and Mohammad Aghababaei Horestani. 2023. A New Ultra-Low-Power High-Order Universal OTA-C Filter Based on CMOS Double Inverters in the Subthreshold Region. Circuits Syst. Signal Process. 42, 11 (Nov 2023), 6379–6398. https://doi.org/10.1007/s00034-023-02401-7

[13] Rezaei, F, "Linearity enhancement in the entire tuning range of CMOS OTA using a new tune compensated source degeneration technique", Microelectronics Journal, 66, 128–135, August 2017. https://doi.org/10.1016/j.mejo.2017.06.008

[14] F. Khateb, T. Kulej, M. Kumngern, and P. Prommee, "0.5-V High-Linear Fully Differential Multiple-Input Bulk-Driven OTA with Effective Self-Embedded Common-Mode Feedback," IEEE Access, vol. 12, pp. 1–1, 2024, doi:10.1109/ACCESS.2024.3389060

[15] Abdolmaleki, M., Dousti, M., & Tavakoli, M. B, "Design and simulation of tunable low-pass Gm-C filter with 1 GHz cutoff frequency based on CMOS inverters for high-speed telecommunication applications", Springer, Analog Integrated Circuits and Signal Processing, 100(2), 279–286, August 2019. https://doi.org/10.1007/s10470-020-01785-9

[16] Lo, T. Y., & Hung, "A 1 GHz equiripple low-pass filter with a high-speed automatic tuning scheme", IEEE Transactions on Very Large Scale Integration (VLSI) Systems, 19(2), 175–181, February 2011. https://doi.org/10.1109/TVLSI.2009.2034527

[17] Rezaei, F& Azhari, "A new controllable adaptive biasing linearization technique for a CMOS OTA nad its application to tunable Gm-c filter design", Microelectronics Journal, 66, 128–135, July 2015. DOI: 10.1016/j.mejo.2015.06.012

[18] Galan, J., Pedro, M., Sanchez-Rodriguez, T., Munoz, "A very linear low-pass filter with automatic frequency tuning", IEEE transactions on Very Large Integration (VLSI) System, January 2013. https://doi.org/10.1109/TVLSI.2011.2181880

[19] Lechevallier, J., Struiksma, R., Sherry, H., Catheli, A., Klum-perink, E, & Nauta, B,"A forward-body-bias tuned450 MHz Gm-C 3rd-order low-pass filter in 28 nm UTBB FD-SOI with [1dBVp IIP3 over a 0.7-to-1V supply",IEEE Inter-national Solid-State Circuits Conference-(ISSCC) Digest of Technical Papers, February 2015. Doi: 10.1109/ISSCC.2015.7062943

[20] Mohammad Abdolmaleki, Massoud Dousti, and Mohammad Bagher Tavakoli. 2021. Design and simulation of fourth order low-pass Gm-C filter with novel auto-tuning circuit in 90 nm CMOS. Analog Integr. Circuits Signal Process. 107, 2 (May 2021), 451–461. https://doi.org/10.1007/s10470-020-01785-9